Modeling of Electrochemical Deionization Across Length Scales: Recent Accomplishments and New Opportunities

Sizhe Liu,[a] Vu Quoc Do,[a] and Kyle C. Smith[a,b,c,d,*]

[a] Department of Mechanical Science and Engineering, University of Illinois at Urbana-Champaign, Urbana, IL 61801, USA

[b] Computational Science and Engineering Program, University of Illinois at Urbana-Champaign, Urbana, IL 61801, USA

[c] Department of Materials Science and Engineering, University of Illinois at Urbana-Champaign, Urbana, IL 61801, USA

[d] Beckman Institute for Advanced Science and Technology, University of Illinois at Urbana-Champaign, Urbana, IL 61801, USA

*corresponding author: kcsmith@illinois.edu

Abstract

Theoretical models have recently been used to simulate deionization technology by capturing electrochemical processes at atomistic, electrode, and plant length scales in electrodialysis, capacitive deionization using electric double layers, and Faradaic deionization using intercalation materials and redox-active polymers. We review the salient features of such models, identifying their major accomplishments in quantifying energy consumption and ion removal, analyzing the feasibility of large-scale systems, and discovering new electrode materials and understanding their deionization mechanisms. By summarizing advantages and disadvantages of recent modeling strategies, we identify research directions to expand modeling capabilities that can be used to inform electrode material/microstructure design, to assign energy losses to electrode-scale mechanisms, to bridge length scales, and to capture Faradaic kinetic/diffusion processes.

Keywords: capacitive deionization; Faradaic deionization; electrodialysis; modeling; multi-scale; intercalation; desalination; water

Introduction

Electrochemical deionization processes use electric fields as a driving force for ion removal, in contrast with pressure- (e.g., reverse osmosis) and temperature-driven (e.g., distillation) processes. While electrodialysis (ED) is by far the most mature deionization process [1], recent research activity has focused on capacitive deionization [2] (CDI) and Faradaic deionization[1] [3] (FDI) processes that use electric charge/discharge cycles to produce deionized and concentrated effluent. Here, we show that models which capture electrochemical processes at various length scales can play an important role in their design and the interpretation of experimental results (Fig. 1). Accordingly, we first review the electrode-scale macrohomogeneous transport models and microscopic electrosorption models. Secondly, we review the plant-scale models that have been used to analyze technical and economic feasibility. Finally, we summarize atomistic models based on molecular dynamics and density functional theory. From this review we identify opportunities for future modeling.

[1] The term *Faradaic* implies that redox occurs in stoichiometric proportion to the current applied to induce electrosorption, thus satisfying Faraday's Law. The term *Faradaic deionization* therefore includes, but is not limited to, electrochemical deionization devices that use ion intercalation materials where the host undergoes redox, polymer materials with redox-active functionalities, and even materials that undergo conversion reactions (e.g., Ag/AgCl and Bi/BiOCl). Though, strictly speaking, the term *Faradaic deionization* includes electrodialysis where solution-phase redox occurs, we refer to electrodialysis separately because of its historical use and its reliance on membrane stacks to effect deionization.

Electrode-scale Modeling

The electrodes in deionization devices have complex porous structures that are filled with electrolyte. During the charge and discharge of such devices, ions transport through macropores and micropores between bulk solution and solid surfaces. Early modeling of porous electrodes investigated the ion transport in macropores by assuming uniform ion concentration in micropores [4] and by treating the solid and electrolyte as superimposed continua [5,6]. These studies identified that deionization performance is dependent on the ion concentration in feed water [7], electrode thickness [8], and the use of ion-exchange membranes (IEMs) [9]. Motivated by the development of novel electrode materials [10,11] and the large-scale application of deionization processes [2], recent modelling research adapted microscopic theories to analyze the influence of pore-scale electrosorption processes and cell architectures on deionization efficiency. These models have included the effects of fluid, ion, and electron transport processes, as well as ion storage by way of electrosorption. In addition, various modelling treats electrodes, membranes, and spacers as macro-homogeneous, where (1) solid and electrolyte are superimposed continua, (2) concentrations are expressed as local volume averaged values, and (3) effective parameters capture microstructure's effect on macro-scale transport.

In CDI ions are adsorbed within electric double-layers (EDLs) near charged electrode surfaces in both micropores and macropores (Fig. 2a). To describe these effects modified Donnan (mD) theory couples micropore ion concentration and potential to those of macropores using a Boltzmann scaling law [9,12,13]. The mD theory has been used to model the influence of electrolyte composition and micropore size on

electrosorption processes [12,14–16]. For example, at high pH the mD theory predicts the prefential electrosorption of counter-ions over co-ions due to increased Donnan potential, in agreement with later experiments [15]. By coupling ion diffusion in bulk solution with electrosorption in micropores, others used mD theory to show that ion adsorption rate is limited by the charge transfer rate between micro- and macro-pores [16]. These results also demonstrated the trade-off between energy consumption and ion removal performance.

Because of its mathematical simplicity the mD theory prevails in deionization research, while careful analysis of experimental data is needed to fit its free parameters [16,17]. However, other EDL theories have been used or introduced recently. Gouy−Chapman−Stern theory predicts the potential drop across the EDL based on the charge imbalance near electrode surfaces. Such theory has been used recently to analyze the energy efficiency of CDI cycles [18,19], while similar analysis has also been performed using mD theory [20]. The dynamic Langmuir theory has also been created to predict the relative adsorption rates for different ions [21] by incorporating “voltage-induced” adsorption sites that have varying affinity toward different ions depending on their size [22]. Also, the effect of the finite size of ions on the selectivity of electrosorption has been explored using the Carnahan-Starling equation [23].

The effects of macrohomogeneous transport have been modeled in a number of recent CDI works, including its coupling to micro-scale electrosorption processes. The first two-dimensional macrohomogeneous transport models of CDI used Nernst-Planck (NP) formulations [12,13]. Later work used models inspired by early CDI modeling [5] to study the effect of introducing macroporous regions into porous electrodes to affect cell

impedance [24] and to model the effects of flow pulsation and side reactions [17]. Other work has explored the effect of conductor percolation on long-range electron conduction in suspensions for flow-electrode CDI [25].

In FDI the oxidation state of a redox-active electrode changes upon electrosorption. Thus, micro-scale models of Faradaic electrosorption processes explicitly track state-of-charge and surface reaction kinetics in a self-consistent manner. Modeling of FDI using cation intercalation materials (Fig. 2b) was first done [8,26,27] by extending porous electrode theory formulations for rechargeable batteries to two-dimensional systems with electrolyte flow [6,28]. These models coupled empirical reaction potentials with local intercalation rates using Butler-Volmer kinetics [8,26,27] for $Na_{0.24+x}MnO_2$, $Na_xTi_2(PO_4)_3$, and $Na_{1+x}NiFe(CN)_6$ (a type of Prussian blue analogue, PBA) together with permselective IEMs having negligible thickness. Such FDI models have been recently used to link desalination energy consumption and salt removal levels to transport mechanisms. FDI cells with non-selective diaphragms between $Na_{1+x}NiFe(CN)_6$ electrodes have also been modeled [27], showing charge efficiency losses that increase with increasing cation transference number in feedwater. Subsequently, theoretical reaction potentials for $Na_{1+x}NiFe(CN)_6$ based on the Frumkin isotherm were modeled in conjunction with a NP formulation and a semi-analytical approach to capture the finite resistance and selecitivity of the IEMs [29]. Concurrent work used similar macrohomogeneous modeling to show that experimental variation of the apparent diffusion coefficients for Na^+ with its degree of intercalation in $Na_{1+x}NiFe(CN)_6$ is the result of sluggish electron conduction within agglomerates of $Na_{1+x}NiFe(CN)_6$ nanoparticles [30]. Such modeling inspired the development of optimized porous electrodes whose performance was simulated to

identify rate-limiting processes in FDI [31], including transverse salt diffusion. Further, the optimization of the electrode material itself was performed by constructing an electrochemical Ashby diagram showing contours of constant performance created using an equivalent circuit model [31]. Beyond cation intercalation materials, a generalized Frumkin-Butler-Volmer theory has been used to model anion capture by redox-active polymers (Fig. 2c) to reproduce the effects of different functional groups and their effect on salt-adsorption capacity [32].

In membrane CDI (MCDI) and ED, IEMs are used to transmit ions selectively, while inducing potential drops across IEMs [33]. Therefore, some models for MCDI and ED use NP formulation with mD theory to model IEMs. For instance, Donnan potential was found to increase with membrane thickness, showing that an optimum IEM thickness for ED removes the most ions from brine [34]. Ion flux through IEMs in MCDI was also modeled implicitly in terms of Donnan potential to find reduced energy consumption in MCDI relative to conventional CDI without IEMs [35] and to quantify the inherent performance/energy tradeoffs in MCDI [36]. A NP formulation was also recently used to directly compare the energy consumption of MCDI and ED, showing lower energy consumption for ED [37]. Others have calculated entropy generation rates based on ion flux through IEMs to analyze ED energy consumption mechanisms [38]. Shock ED processes have also been modeled based on a one-dimensional NP formulation, focusing on fluidic instabilities induced by electric fields [39]. Electroconvective vortices have also been modeled in ED channels using a NP formulation [40]. Because the coupled differential equations in the NP formulation pose challenges to numerical implementation, other work has sought to simplify ED stack models using resistor-capacitor (RC) networks

to predict current and flux distributions [41], enabling integration of such processes into plant-scale models [42].

While most previous ED modeling has imposed periodic, isopotential conditions at terminal IEMs (following early ED modeling [7]), recent modeling of ED-like cells using either soluble [43] or solid [26] redox-active materials has explicitly resolved reaction rates within electrodes. In particular, the coupled power production and desalination performance of an ED cell with a single diluate and concentrate stream were simulated [43]. In addition desalination energy consumption has been shown to increase substantially for ED stacks of increasing size that use $Na_{1+x}NiFe(CN)_6$ intercalation electrodes, as a result of the non-uniform current distribution [26].

Plant-scale Modeling

Analysis of the economic and technical feasibility of deionization technology has recently leveraged plant-scale models that mathematically simplify the relationships between design/operating parameters and performance metrics. CDI flow chambers were modeled using Randles circuits, where macroscopic ion transfer effects were described using electrochemical impedance [44]. Using this approach the authors later compared the predicted salt removal efficiency of CDI, ED, and RO cells, concluding that CDI has certain limitations on energy efficiency. A subsequent critique of that work argued that simplistic Randles circuits are incapable of predicting cell resistance accurately, resulting in unphysical values of thermodynamic efficiency and energy consumption [45]. In response, the authors of the original study used a NP formulation

to ultimately show similar scaling of energy efficiency with average water flux [46] as their original Randles circuit. Other work established a theoretical design framework developed for MCDI plants to predict performance/energy-consumption tradeoffs [47]. The sensitivity of energy consumption and water recovery to individual CDI design/operating parameters has also been analyzed using one-dimensional models [48]. Subsequently, CDI modules were modeled as ideal capacitors to design a multi-channel cell [49], showing that the charge efficiency of electrodes has a significant impact on cost.

Atomistic Modeling

While continuum models are significantly less computationally intensive than atomistic models, atomistic models enable the discovery of electrochemical phenomena with little-to-no mechanistic understanding *a priori*. As such, atomistic modeling is an important future direction for deionization materials and devices. Two methods have been used commonly in these contexts: molecular dynamics (MD) and density functional theory (DFT). In MD simulations predefined electric fields generate potential energies for individual atoms that ultimately dictate their time-dependent dynamics. In contrast, DFT is used to simulate the ground-state electronic structure of various atomic arrangements.

MD simulations have recently been used to model electrosorption processes in nanostructured materials. In particular, the hydration structure of ions near graphitic electrodes was modeled using first-principles MD in conjunction with experiments [50,51]. Here, the reference interaction site model [52] was used to predict ion hydration energy, showing that asymmetric hydration shells can reduce hydration energy and speed up

electrosorption processes. Stable water shells have also been found to increase in size with decreasing nanopore size, while water-filled pores were shown to be ionophobic and remained inactive during charging processes [53]. Other work has used MD to model an ion/molecule separations process between flat electrodes [54]. Here, the electric field between the electrodes acts as an additional force on each atom. Seawater flow between corrugated electrodes was also recently simulated using MD, showing higher ion adsorption rate on uneven electrodes [55].

While MD simulations are highly scalable to large numbers of atoms, they often require empirical parameters to compute pairwise potential energies and forces that do not explicitly capture electronic degrees of freedom. As a result, for Faradaic electrosorption materials [56] the use of pairwise potential energies is limited. In contrast, DFT is a self-consistent method that explicitly captures atomic interactions via coulomb interactions with the spatial distribution of electron density. Along these lines DFT has been used to analyze interactions between anions at ferrocene groups on polyvinyl ferrocene electrodes [57]. The charge distribution on ferrocene was found to distort towards CrO_4^{2-} and $HAsO_4^{2-}$ ions, an atomic affinity effect that was attributed to electron transfer toward ferrocene. Other work using DFT has shown decreased band gaps for zwitterionic-polymer CDI electrodes when multivalent ions adsorb [58].

DFT has also been used in recent research to link electrode response to changes in electronic structure. For example, certain metal-organic framework (MOF) electrodes transform into insulators during charging processes [59]. To explain this phenomenon, electron density distributions were simulated at various degrees of intercalation, and π-stacking interactions between organic ligands were found to vanish with increasing

degree of intercalation. DFT has also been combined with experiment to link the capacity fade and retention of PBA materials to the substitution of Ni^{2+} metal centers by Mg^{2+} and Ca^{2+} ions in solution [60]. In addition, that analysis revealed that such substitutions introduce discontinuities in the electron density distributions of PBA frameworks. These findings from DFT were subsequently used to construct a network model of electron transmission to predict the charge storage capacity of a PBA material as a function of the fraction of Ni^{2+} sites substituted.

Because DFT calculates the ground-state of electrons at $T = 0\ K$, other physics-based techniques can be used to analyze finite-temperature, non-equilibrium effects using ground-state energetics. DFT was used to show that vacancy-vacancy interactions within the interstitial sites of PBAs result in ordering of intercalated Na^+ [61]. Based on this finding a simplified model was developed that assigned infinite energy to pairs of nearest neighbor vacancies, enabling the prediction of equilibrium potential for Na^+ intercalation versus state-of-charge using a grand canonical ensemble formalism. The influence of H_2O on Zn-ion diffusion in bilayer V_2O_5 has been investigated using DFT [62], revealing a reduced binding energy between cations and V_2O_5 sheets due to a charge shielding effect caused by electron-accepting H_2O molecules.

Conclusion and Outlook

Recent work in the modeling of electrochemical deionization systems has certain advantages and disadvantages depending on the length scale of interest (Table 1). To expand modeling capabilities we highlight the following future research directions (Fig. 1):

- Electrode-scale models can adopt methods of exergy destruction [63] and entropy generation [38] analysis to quantify local, instantaneous energy dissipation rates from the diversity of processes that occur in electrochemical systems. Such analysis can enable the targeted development and optimization of specific cell components and materials.

- The modeling of electrochemical kinetics and solid-state diffusion in FDI electrodes could be used to select, design, and analyze energy-consumption/selectivity of electrode materials for FDI.

- Connections between electrode microstructure and electrode-scale transport can be made using pore- and microstructure-resolved models [25,64], as mD theory relies on uniform-concentration/potential assumptions [9,12,13] and macrohomogeneous models rely on phenomenological force/flux relations for forced convection in porous electrodes [8,26,27,31].

- Machine learning approaches can be used to accelerate material discovery [65] due to the computational limitations of large-scale DFT calculations [66], while also enabling bridging between electrode- and plant-scale models in combination with reduced order models.

- Materials genome approaches can be used to search for water-stable FDI electrode materials (cf. Ref. [67]), while combining such results with statistical thermodynamics to define and discover mechanisms for specific CDI/FDI materials to create electrode-scale models including solvent interactions.

Acknowledgments

This work was supported by the US National Science Foundation (Award No. 1931659).

References

[1] H. Strathmann, Electrodialysis, a mature technology with a multitude of new applications, Desalination. 264 (2010) 268–288. doi:10.1016/j.desal.2010.04.069.

[2] M.E. Suss, S. Porada, X. Sun, P.M. Biesheuvel, J. Yoon, V. Presser, Water desalination via capacitive deionization: what is it and what can we expect from it?, Energy Environ. Sci. 8 (2015) 2296–2319. doi:10.1039/C5EE00519A.

[3] W. Tang, J. Liang, D. He, J. Gong, L. Tang, Z. Liu, D. Wang, G. Zeng, Various cell architectures of capacitive deionization: Recent advances and future trends, Water Res. 150 (2019) 225–251. doi:10.1016/j.watres.2018.11.064.

[4] E.H. Cwirko, R.G. Carbonell, A theoretical analysis of donnan dialysis across charged porous membranes, J. Memb. Sci. 48 (1990) 155–179. doi:10.1016/0376-7388(90)85003-4.

[5] A.M. Johnson, J. Newman, Desalting by Means of Porous Carbon Electrodes, J. Electrochem. Soc. 118 (1971) 510–517. doi:10.1149/1.2408094.

[6] W. Lai, F. Ciucci, Mathematical modeling of porous battery electrodes—Revisit of Newman's model, Electrochim. Acta. 56 (2011) 4369–4377. doi:10.1016/j.electacta.2011.01.012.

[7] A.A. Sonin, R.F. Probstein, A hydrodynamic theory of desalination by electrodialysis, Desalination. 5 (1968) 293–329. doi:10.1016/S0011-9164(00)80105-8.

[8] K.C. Smith, R.D. Dmello, Na-Ion Desalination (NID) Enabled by Na-Blocking Membranes and Symmetric Na-Intercalation: Porous-Electrode Modeling, J. Electrochem. Soc. 163 (2016) A530–A539. doi:10.1149/2.0761603jes.

[9] P.M. Biesheuvel, R. Zhao, S. Porada, A. van der Wal, Theory of membrane capacitive deionization including the effect of the electrode pore space, J. Colloid Interface Sci. 360 (2011) 239–248. doi:10.1016/j.jcis.2011.04.049.

[10] Y. Cheng, Z. Hao, C. Hao, Y. Deng, X. Li, K. Li, Y. Zhao, A review of modification of carbon electrode material in capacitive deionization, RSC Adv. 9 (2019) 24401–24419. doi:10.1039/c9ra04426d.

[11] A.G. El-Deen, J.H. Choi, C.S. Kim, K.A. Khalil, A.A. Almajid, N.A.M. Barakat, TiO2 nanorod-intercalated reduced graphene oxide as high performance electrode material for membrane capacitive deionization, Desalination. 361 (2015) 53–64. doi:10.1016/j.desal.2015.01.033.

[12] A. Hemmatifar, M. Stadermann, J.G. Santiago, Two-Dimensional Porous Electrode Model for Capacitive Deionization, J. Phys. Chem. C. 119 (2015) 24681–24694. doi:10.1021/acs.jpcc.5b05847.

[13] S. Porada, L. Borchardt, M. Oschatz, M. Bryjak, J.S. Atchison, K.J. Keesman, S. Kaskel, P.M. Biesheuvel, V. Presser, Direct prediction of the desalination performance of porous carbon electrodes for capacitive deionization, Energy Environ. Sci. 6 (2013) 3700–3712. doi:10.1039/c3ee42209g.

[14] Y. Qu, P.G. Campbell, A. Hemmatifar, J.M. Knipe, C.K. Loeb, J.J. Reidy, M.A. Hubert, M. Stadermann, J.G. Santiago, Charging and Transport Dynamics of a Flow-Through Electrode Capacitive Deionization System, J. Phys. Chem. B. 122 (2018) 240–249. doi:10.1021/acs.jpcb.7b09168.

[15] A. Hemmatifar, D.I. Oyarzun, J.W. Palko, S.A. Hawks, M. Stadermann, J.G. Santiago, Equilibria model for pH variations and ion adsorption in capacitive deionization electrodes, Water Res. 122 (2017) 387–397. doi:10.1016/j.watres.2017.05.036.

[16] Y. Salamat, C.H. Hidrovo, Significance of the micropores electro-sorption resistance in capacitive deionization systems, Water Res. 169 (2020). doi:10.1016/j.watres.2019.115286.

[17] X. Shang, R.D. Cusick, K.C. Smith, A Combined Modeling and Experimental Study Assessing the Impact of Fluid Pulsation on Charge and Energy Efficiency in Capacitive Deionization, J. Electrochem. Soc. 164 (2017) E536–E547. doi:10.1149/2.0841714jes.

[18] D. Moreno, M.C. Hatzell, Efficiency of Carnot and Conventional Capacitive Deionization Cycles, J. Phys. Chem. C. 122 (2018) 22480–22486. doi:10.1021/acs.jpcc.8b05940.

[19] A. Hemmatifar, A. Ramachandran, K. Liu, D.I. Oyarzun, M.Z. Bazant, J.G. Santiago, Thermodynamics of Ion Separation by Electrosorption, Environ. Sci. Technol. 52 (2018) 10196–10204. doi:10.1021/acs.est.8b02959.

[20] L. Wang, P.M. Biesheuvel, S. Lin, Reversible thermodynamic cycle analysis for capacitive deionization with modified Donnan model, J. Colloid Interface Sci. 512 (2018) 522–528. doi:10.1016/j.jcis.2017.10.060.

[21] J. Nordstrand, J. Dutta, Simplified Prediction of Ion Removal in Capacitive Deionization of Multi-Ion Solutions, Langmuir. (2020) acs.langmuir.9b03571. doi:10.1021/acs.langmuir.9b03571.

[22] J. Nordstrand, J. Dutta, Dynamic Langmuir Model: A Simpler Approach to Modeling Capacitive Deionization, J. Phys. Chem. C. 123 (2019) 16479–16485.

doi:10.1021/acs.jpcc.9b04198.

[23] E.N. Guyes, T. Malka, M.E. Suss, Enhancing the ion-size-based selectivity of capacitive deionization electrodes, Environ. Sci. Technol. 53 (2019) 8447–8454. doi:10.1021/acs.est.8b06954.

[24] E.R. Reale, K.C. Smith, Capacitive Performance and Tortuosity of Activated Carbon Electrodes with Macroscopic Pores, J. Electrochem. Soc. 165 (2018) A1685–A1693. doi:10.1149/2.0601809jes.

[25] M. Karzar-Jeddi, H. Luo, P.T. Cummings, K.B. Hatzell, Computational Modeling of Particle Hydrodynamics and Charging Process for the Flowable Electrodes of Carbon Slurry, J. Electrochem. Soc. 166 (2019) A2643–A2653. doi:10.1149/2.1191912jes.

[26] K.C. Smith, Theoretical evaluation of electrochemical cell architectures using cation intercalation electrodes for desalination, Electrochim. Acta. 230 (2017) 333–341. doi:10.1016/j.electacta.2017.02.006.

[27] S. Liu, K.C. Smith, Quantifying the Trade-offs between Energy Consumption and Salt Removal Rate in Membrane-free Cation Intercalation Desalination, Electrochim. Acta. 271 (2018) 652–665. doi:10.1016/j.electacta.2018.03.065.

[28] T.F. Fuller, Simulation and Optimization of the Dual Lithium Ion Insertion Cell, J. Electrochem. Soc. 141 (1994) 1. doi:10.1149/1.2054684.

[29] K. Singh, H.J.M. Bouwmeester, L.C.P.M. de Smet, M.Z. Bazant, P.M. Biesheuvel, Theory of Water Desalination with Intercalation Materials, Phys. Rev. Appl. 9 (2018) 064036. doi:10.1103/PhysRevApplied.9.064036.

[30] A. Shrivastava, K.C. Smith, Electron Conduction in Nanoparticle Agglomerates Limits Apparent Na+ Diffusion in Prussian Blue Analogue Porous Electrodes, J. Electrochem. Soc. 165 (2018) A1777–A1787. doi:10.1149/2.0861809jes.

[31] E.R. Reale, A. Shrivastava, K.C. Smith, Effect of conductive additives on the transport properties of porous flow-through electrodes with insulative particles and their optimization for Faradaic deionization, Water Res. 165 (2019) 114995. doi:10.1016/j.watres.2019.114995.

[32] F. He, P.M. Biesheuvel, M.Z. Bazant, T.A. Hatton, Theory of water treatment by capacitive deionization with redox active porous electrodes, Water Res. 132 (2018) 282–291. doi:10.1016/j.watres.2017.12.073.

[33] A. Campione, L. Gurreri, M. Ciofalo, G. Micale, A. Tamburini, A. Cipollina, Electrodialysis for water desalination: A critical assessment of recent developments on process fundamentals, models and applications, Desalination. 434 (2018) 121–160. doi:10.1016/j.desal.2017.12.044.

[34] M. Tedesco, H.V.M. Hamelers, P.M. Biesheuvel, Nernst-Planck transport theory for (reverse) electrodialysis: III. Optimal membrane thickness for enhanced process performance, J. Memb. Sci. 565 (2018) 480–487. doi:10.1016/j.memsci.2018.07.090.

[35] T.M. Mubita, S. Porada, P.M. Biesheuvel, A. van der Wal, J.E. Dykstra, Capacitive deionization with wire-shaped electrodes, Electrochim. Acta. 270 (2018) 165–173. doi:10.1016/j.electacta.2018.03.082.

[36] L. Wang, S. Lin, Intrinsic tradeoff between kinetic and energetic efficiencies in membrane capacitive deionization, Water Res. 129 (2018) 394–401. doi:10.1016/j.watres.2017.11.027.

[37] S.K. Patel, M. Qin, W.S. Walker, M. Elimelech, Energy Efficiency of Electro-Driven Brackish Water Desalination: Electrodialysis Significantly Outperforms Membrane Capacitive Deionization, Environ. Sci. Technol. 54 (2020) 3663–3677. doi:10.1021/acs.est.9b07482.

[38] K.M. Chehayeb, J.H. Lienhard, Entropy generation analysis of electrodialysis, Desalination. 413 (2017) 184–198. doi:10.1016/j.desal.2017.03.001.

[39] Z. Gu, B. Xu, P. Huo, S.M. Rubinstein, M.Z. Bazant, D. Deng, Deionization shock driven by electroconvection in a circular channel, Phys. Rev. Fluids. 4 (2019) 1–11. doi:10.1103/PhysRevFluids.4.113701.

[40] J. Yoon, V.Q. Do, V.S. Pham, J. Han, Return flow ion concentration polarization desalination: A new way to enhance electromembrane desalination, Water Res. 159 (2019) 501–510. doi:10.1016/j.watres.2019.05.042.

[41] A. Campione, A. Cipollina, E. Toet, L. Gurreri, I.D.L. Bogle, G. Micale, Water desalination by capacitive electrodialysis: Experiments and modelling, Desalination. 473 (2020) 114150. doi:10.1016/j.desal.2019.114150.

[42] A. Campione, A. Cipollina, I.D.L. Bogle, L. Gurreri, A. Tamburini, M. Tedesco, G. Micale, A hierarchical model for novel schemes of electrodialysis desalination, Desalination. 465 (2019) 79–93. doi:10.1016/j.desal.2019.04.020.

[43] I. Atlas, M.E. Suss, Theory of simultaneous desalination and electricity generation via an electrodialysis cell driven by spontaneous redox reactions, Electrochim. Acta. 319 (2019) 813–821. doi:10.1016/j.electacta.2019.06.014.

[44] M. Qin, A. Deshmukh, R. Epsztein, S.K. Patel, O.M. Owoseni, W.S. Walker, M. Elimelech, Comparison of energy consumption in desalination by capacitive deionization and reverse osmosis, Desalination. 455 (2019) 100–114. doi:10.1016/j.desal.2019.01.003.

[45] A. Ramachandran, D.I. Oyarzun, S.A. Hawks, P.G. Campbell, M. Stadermann, J.G. Santiago, Comments on “Comparison of energy consumption in desalination by capacitive deionization and reverse osmosis,” Desalination. 461 (2019) 30–36. doi:10.1016/j.desal.2019.03.010.

[46] M. Qin, A. Deshmukh, R. Epsztein, S.K. Patel, O.M. Owoseni, W.S. Walker, M. Elimelech, Response to comments on “Comparison of energy consumption in desalination by capacitive deionization and reverse osmosis,” Desalination. 462 (2019) 48–55. doi:10.1016/j.desal.2019.04.004.

[47] L. Wang, S. Lin, Theoretical framework for designing a desalination plant based

on membrane capacitive deionization, Water Res. 158 (2019) 359–369. doi:10.1016/j.watres.2019.03.076.

[48] S. Hand, X. Shang, J.S. Guest, K.C. Smith, R.D. Cusick, Global sensitivity analysis to characterize operational limits and prioritize performance goals of capacitive deionization, Environ. Sci. Technol. 53 (2019) 3748–3756. doi:10.1021/acs.est.8b06709.

[49] S. Hand, J.S. Guest, R.D. Cusick, Technoeconomic Analysis of Brackish Water Capacitive Deionization: Navigating Tradeoffs between Performance, Lifetime, and Material Costs, Environ. Sci. Technol. 53 (2019) 13353–13363. doi:10.1021/acs.est.9b04347.

[50] S.A. Hawks, M.R. Cerón, D.I. Oyarzun, T.A. Pham, C. Zhan, C.K. Loeb, D. Mew, A. Deinhart, B.C. Wood, J.G. Santiago, M. Stadermann, P.G. Campbell, Using Ultramicroporous Carbon for the Selective Removal of Nitrate with Capacitive Deionization, Environ. Sci. Technol. 53 (2019) 10863–10870. doi:10.1021/acs.est.9b01374.

[51] C. Zhan, M.R. Cerón, S.A. Hawks, M. Otani, B.C. Wood, T.A. Pham, M. Stadermann, P.G. Campbell, Specific ion effects at graphitic interfaces, Nat. Commun. 10 (2019) 1–8. doi:10.1038/s41467-019-12854-7.

[52] S. Tanimoto, N. Yoshida, T. Yamaguchi, S.L. Ten-no, H. Nakano, Effect of Molecular Orientational Correlations on Solvation Free Energy Computed by Reference Interaction Site Model Theory, J. Chem. Inf. Model. 59 (2019) 3770–3781. doi:10.1021/acs.jcim.9b00330.

[53] S. Bi, Y. Zhang, L. Cervini, T. Mo, J.M. Griffin, V. Presser, G. Feng, Permselective ion electrosorption of subnanometer pores at high molar strength enables capacitive deionization of saline water, Sustain. Energy Fuels. (2020). doi:10.1039/c9se00996e.

[54] F. Sofos, T.E. Karakasidis, D. Spetsiotis, Molecular dynamics simulations of ion separation in nano-channel water flows using an electric field, Mol. Simul. 45 (2019) 1395–1402. doi:10.1080/08927022.2019.1637520.

[55] M. Dahanayaka, B. Liu, Z. Hu, Z. Chen, A.W.K. Law, K. Zhou, Corrugated graphene layers for sea water desalination using capacitive deionization, Phys. Chem. Chem. Phys. 19 (2017) 8552–8562. doi:10.1039/c7cp00389g.

[56] S. Fleischmann, A. Tolosa, M. Zeiger, B. Krüner, N.J. Peter, I. Grobelsek, A. Quade, A. Kruth, V. Presser, Vanadia-titania multilayer nanodecoration of carbon onions via atomic layer deposition for high performance electrochemical energy storage, J. Mater. Chem. A. 5 (2017) 2792–2801. doi:10.1039/c6ta09890h.

[57] X. Su, A. Kushima, C. Halliday, J. Zhou, J. Li, T.A. Hatton, Electrochemically-mediated selective capture of heavy metal chromium and arsenic oxyanions from water, Nat. Commun. 9 (2018). doi:10.1038/s41467-018-07159-0.

[58] Y. Jung, Y. Yang, T. Kim, H.S. Shin, S. Hong, S. Cha, S. Kwon, Enhanced

Electrochemical Stability of a Zwitterionic-Polymer-Functionalized Electrode for Capacitive Deionization, ACS Appl. Mater. Interfaces. 10 (2018) 6207–6217. doi:10.1021/acsami.7b14609.

[59] N. Ogihara, N. Ohba, Y. Kishida, On/off switchable electronic conduction in intercalated metal-organic frameworks, Sci. Adv. 3 (2017) e1603103. doi:10.1126/sciadv.1603103.

[60] A. Shrivastava, S. Liu, K.C. Smith, Linking capacity loss and retention of nickel hexacyanoferrate to a two-site intercalation mechanism for aqueous Mg2+ and Ca2+ ions, Phys. Chem. Chem. Phys. 21 (2019) 20177. doi:10.1039/c9cp04115j.

[61] S. Liu, K.C. Smith, Intercalated Cation Disorder in Prussian Blue Analogues: First-Principles and Grand Canonical Analyses, J. Phys. Chem. C. 123 (2019) 10191–10204. doi:10.1021/acs.jpcc.8b12455.

[62] T. Wu, K. Zhu, C. Qin, K. Huang, Unraveling the role of structural water in bilayer V2O5 during Zn2+-intercalation: Insights from DFT calculations, J. Mater. Chem. A. 7 (2019) 5612–5620. doi:10.1039/c8ta12014e.

[63] V.P. Nemani, K.C. Smith, Assignment of Energy Loss Contributions in Redox Flow Batteries using Exergy Destruction Analysis, J. Power Sources. 447 (2020) 227371. doi:10.1016/j.jpowsour.2019.227371.

[64] M.A. Hamid, K.C. Smith, Modeling the Transient Effects of Pore-Scale Convection and Redox Reactions in the Pseudo-Steady Limit, J. Electrochem. Soc. 167 (2020) 013521. doi:10.1149/2.0212001JES.

[65] R.P. Joshi, J. Eickholt, L. Li, M. Fornari, V. Barone, J.E. Peralta, Machine Learning the Voltage of Electrode Materials in Metal-Ion Batteries, ACS Appl. Mater. Interfaces. 11 (2019) 18494–18503. doi:10.1021/acsami.9b04933.

[66] W. Zhang, P. Sun, S. Sun, A precise theoretical method for high- throughput screening of novel organic electrode materials for Li-ion batteries, J. Mater. 3 (2017) 184–190. doi:10.1016/j.jmat.2016.11.009.

[67] X. Zhang, Z. Zhang, S. Yao, A. Chen, X. Zhao, Z. Zhou, An effective method to screen sodium-based layered materials for sodium ion batteries, Npj Comput. Mater. 4 (2018). doi:10.1038/s41524-018-0070-2.

Table 1. Summary of the advantages and disadvantages of recent multi-scale modeling strategies.

Length Scale	Advantages	Disadvantages
Atomistic	• Reveals emergent effects of interactions between electrons, ions, and solvent; • Explains electrosorption selectivity mechanisms for various electrode materials; • Potential to inform material design.	• Computationally intensive; • Lack of accurate inter-atomic potentials; • Combinatorial “explosion” occurs in analysis of defect chemistry.
Electrode-scale	• Macrohomogeneous description captures long-range transport processes efficiently; • Identification of rate- and selectivity-limiting processes and conditions; • Quantify tradeoffs between energy consumption and ion removal rate.	• Simplified description of microstructures does not inform material design; • Semi-empirical formulas adopted for surface reaction kinetics and equilibrium; • Sometimes difficult to incorporate in plant-scale models.
Plant-scale	• Design at plant-scale for various deionization technologies; • Analysis of long-term performance of deionization processes.	• Heuristic formulation can lead to physically inconsistent results; • Macrohomogeneous transport processes are largely ignored.

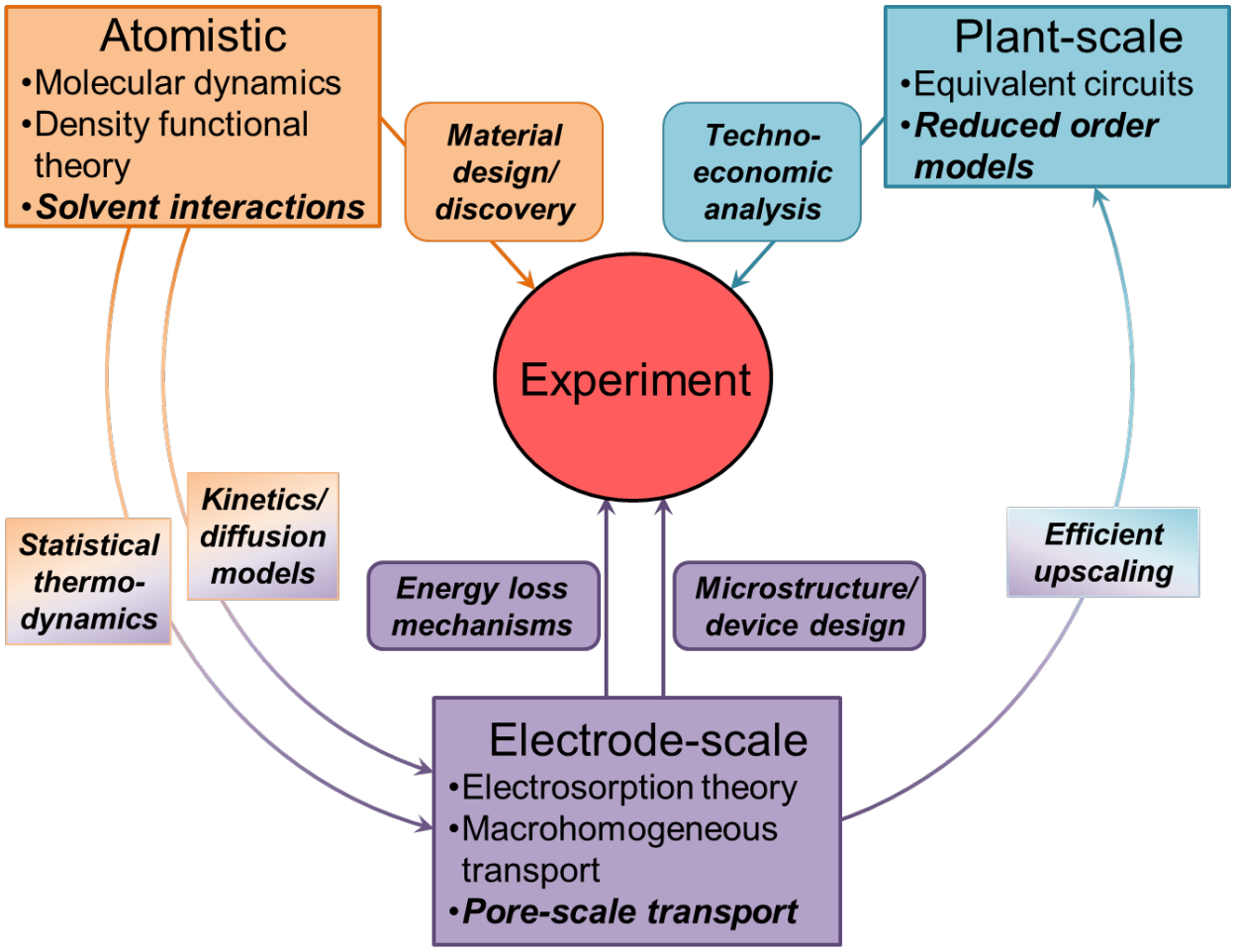

Figure 1. Organization of and vision for multi-scale modeling of electrochemical deionization processes. Items in ***bold italics*** represent new and emerging modeling opportunities at different scales and between scales.

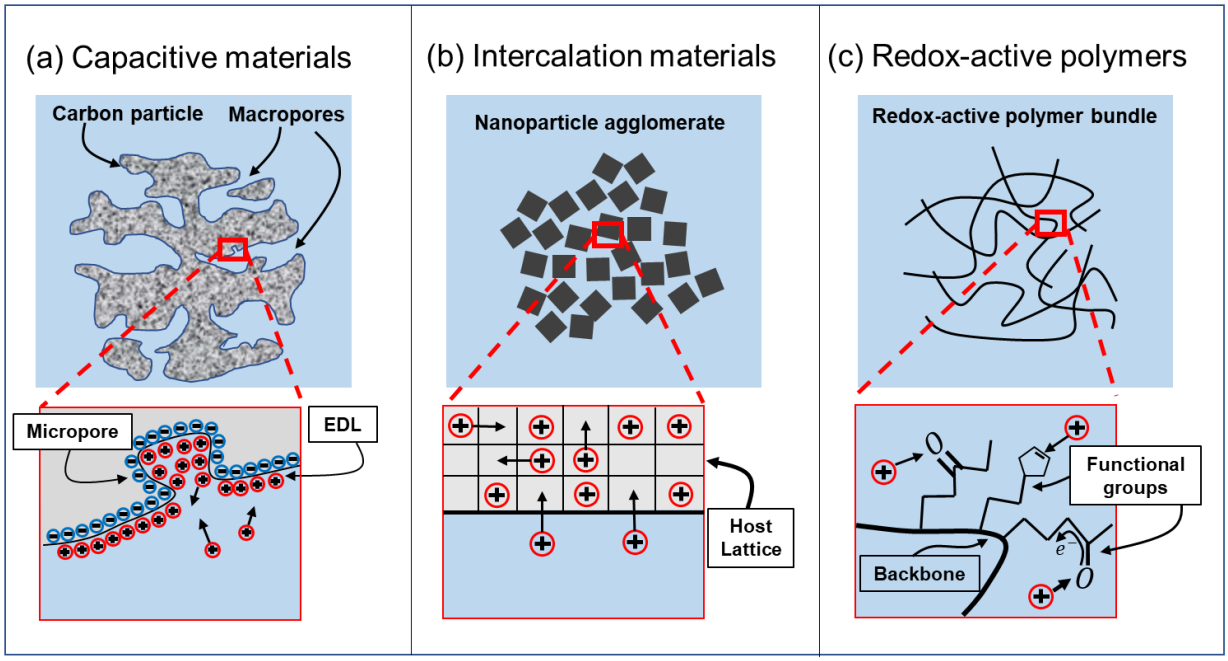

Figure 2. Schematic of the different electrosorption mechanisms that have recently been modeled: (a) a capacitive material builds up electric double layer to capture ions, (b) cations intercalate into the lattice of a redox-active solid host, and (c) functional groups on a redox-active polymer adsorb ions.